Industry Science and Engineering Vol. 3 No. 7, 2026

Determination of Nickel, Cobalt and Manganese in Lithium Nickel–Cobalt–Manganese Oxide Battery Materials by X-Ray Fluorescence Spectrometry with Fusion Preparation

Lei Yu[1,2], Yuting Zuo[1], Xiao Zhang[1,2,*], Yin Yang[1], Tian Li[1,2], Li Wang[2,*], Ruixin Liu[2]
[1]*China United Test & Certification Co., Ltd., Beijing, China*
[2]*Guobiao (Beijing) Testing & Certification Co., Ltd., Beijing, China*
**Corresponding Author*

Abstract: This study established a rapid method for the simultaneous determination of nickel, cobalt, and manganese in lithium nickel–cobalt–manganese oxide (NMC). Sample preparation employed fusion pretreatment using a mixed flux of lithium tetraborate and lithium metaborate (67:33 mass ratio), followed by pre-oxidation at 700 °C for 10 min, fusion at 1150 °C, and artificial synthesis of calibration standards with well-defined concentration gradients from high-purity reference reagents. Quantitative analysis was performed using a wavelength-dispersive X-ray fluorescence (WDXRF) spectrometer. Key analytical parameters—including flux composition, flux-to-sample dilution ratio, excitation voltage and current, and matrix correction-were systematically optimized. Under the optimized conditions, certified reference materials were analyzed. The measured values fell within the certified uncertainty intervals, and the relative standard deviation (RSD) for replicate analyses was less than 2%. The results demonstrate that this method is rapid, accurate, and fully suitable for quality control analysis of lithium nickel–cobalt–manganese oxide battery materials.

Keywords: Lithium Nickel Cobalt Manganate; Cathode Battery Material; X-Ray Fluorescence Spectrometry; Fusion Preparation

1. Introduction

Since the advent of the first lithium-ion battery, lithium-ion battery technology has developed rapidly [1,2]. Owing to its safety, environmental compatibility, high energy capacity, high output power, low self-discharge rate, and other advantages, it is widely used in portable electronic devices, medical equipment, and other fields [3-5]. Among cathode materials for lithium-ion batteries, high-nickel ternary cathodes-NCM ($LiNixCoyMnzO_2$) and NCA (LiNixCoyAlzO2, where x+y+z = 1) -offer superior energy density and dominate the power battery market [6-8]. Electrochemical performance is a key performance indicator of lithium-ion battery cathode materials [9]. Studies have shown a close correlation between the electrochemical performance of lithium nickel–cobalt–manganese oxide (NMC) and its elemental composition. For instance, NMC materials with higher nickel content exhibit greater specific capacity but poorer cycling stability; conversely, those with higher cobalt and manganese content show improved cycling performance but reduced specific capacity [10-12]. Therefore, precise control of the stoichiometric ratios of functional elements (Ni, Co, Mn) and the concentrations of detrimental impurity elements in NMC is critically important to ensure the electrochemical performance, service life, and safety of lithium-ion batteries [13-15].

At present, the primary analytical methods for lithium nickel–cobalt–manganese oxide (NMC) battery materials are inductively coupled plasma optical emission spectrometry (ICP-OES) and classical wet chemical methods [16,17]. The nickel element is determined by the dimethyl ketone gravimetric method, which is a classic chemical method. Luo et al. [18] employed ICP-OES to determine the concentrations of lithium, nickel, cobalt, and manganese in spent secondary battery waste. Wu et al. [19] applied ICP-AES to quantify thirteen impurity elements in lithium cobalt oxide, lithium nickel–cobalt–manganese oxide, lithium carbonate, manganese dioxide, and cobalt tetroxide. The Chinese standard YS/T 1006–2014, “Chemical Analysis

Methods for Lithium Nickel–Cobalt–Manganese Oxide", Part 1 uses titrimetric analysis to determine the total content of major elements, while Part 2 employs ICP-OES for impurity element quantification.

However, applications of X-ray fluorescence spectrometry (XRF) to NMC battery materials remain limited. XRF offers distinct advantages—including rapid analysis, high accuracy, broad elemental coverage (typically Na to U), wide linear dynamic range, and simultaneous multi-element detection—and is widely used for quality control of raw materials, auxiliaries, and finished products such as steel, alloys, ores, and advanced energy materials. When samples are prepared as homogeneous fused glass discs, matrix and particle-size effects are significantly minimized, thereby improving measurement accuracy. In this study, NMC battery materials were converted into uniform glass discs via fusion, and the main elemental composition (Ni, Co, Mn, and Li) of lithium nickel–cobalt–manganese oxide was determined using wavelength-dispersive XRF (WD-XRF).

2. Experimental

2.1 Instrument and Reagents

We used a Zetium-model wavelength-dispersive X-ray fluorescence spectrometer as the analytical instrument, which was produced by Malvern Panalytical. A melting furnace of TD4-modelused to prepare glass discs, and the melting furnaceis produced by Luoyang Haina Testing Instrument Co., Ltd. Additionally, the study used a electric blast-drying oven to dry the samples, the instrument produced by Tianjin Zhonghuan Electric Furnace Co., Ltd. A platinum-gold crucible (95% Pt and 5% Au) was the crucible specifically used for the XRF method.

We used a mixed flux (67% lithium tetraborate and 33% lithium metaborate; highly pure) purchased from Luoyang Tenak High-Temperature Instrument Equipment Co., Ltd., this flux need to heated at 700 °C for 2 h and cooded to room temperature ,then placed it in a desiccator. The lithium bromide solution (concentration 30%); The cobalt tetroxide, manganese dioxide and nickel oxide (>99.99%) purchased from Gangyan Nanoke Testing Technology Co., Ltd. The lithium oxide (>99.99%) purchased from Ding Reagent Co., Ltd. heated at 105 °C for 2 hours and and cooded to room temperature, the placed in the desiccator.

2.2 Instrumental Conditions

The Zetium-model wavelength dispersive X-ray fluorescence spectrometer from PANalytical was used in this study, controlled by the superQ software. The woking conditions for nickel, cobalt and manganese in lithium nickel–cobalt–manganese oxide battery materials are shown in Table 1.

Table 1. Instrumental Conditions

Element	Line	kV	mA	Crystal	Collimator
Ni	Kα	60	60	LiF220	150μm
Co	Kα	60	60	LiF200	150μm
Mn	Kα	60	60	LiF200	150μm

2.3 Preparation of Sample

Weighed 0.6000 ± 0.0001 g of sample and 10.0000 ± 0.0005 g of lithium tetraborate–lithium metaborate mixed flux into a Pt–Au crucible, mixed them well using a fine glass rod and added about five drops of lithium bromide solution. Placed the crucible into the sample melting furnace for melting. The melting is carried out by gradient heating to prevent lithium oxide from splashing. After gradually heating to 700 °C and holding for10 minutes, the temperature is increased to 1150 °C, and melting continues for 17 minutes under rocking conditions. After the melting is completed, the meltis cooled to room temperature under controlled conditions and carefully demolded, and stored in a desiccator.

2.4 Preparation of Calibration Samples

According to the preset mass fraction of each element, the pretreated components-cobalt tetroxide, manganese dioxide, nickel oxide and lithium oxide are weighed in a specific proportion and homogeneously mixed. Standard glass reference materials for each component are then prepared.

In addition to the elements to be measured (nickel, cobalt and manganese), lithium oxide need to be added to ensure matrix consistency with the actual sample matrix. According to the above melting steps, a standard sample with a certain gradient is prepared to draw a standard curve. The content range of each element in the standard sample see Table 2 below.

Table 2. Series of Standard Sample Element Contents (%)

	NiO	Co_3O_4	MnO_2	Li_2O
Scope(%)	5.00-80.00	5.00-50.00	1.00-48.00	1.00-30.00

2.5 Drawing Calibration Curves and Setting Drift Correction

Established the quantitative analysis program, under the measurement conditions of the instrument, measured the intensities of the calibration sample's spectral lines, background, and interference line. Then we obtain the net intensities of each element's spectral lines in the calibration sample. Taking the mass fraction of the measured element as the abscissa, and the X-ray fluorescence intensity as the ordinate, ploting the working curve, and based on the situation of the curve. Usually select the theoretical alpha coefficient method or fundamental parameter method to correct inter-element absorption and enhancement effects, and apply appropriate correction coefficients to establish the calibration curve.

While drawing the calibration curve, set up the monitoring sample, measure the X-ray fluorescence intensity of the analytes in the monitoring sample, and record the initial measurement intensity for subsequent instrument drift calibration. To ensure the effectiveness of drift calibration, the initial measurement of the monitoring sample and the measurement of the standard reference material should be completed within the same time period. A single-point or two-point calibration may be used, and the time interval should be determined according to the instrument's stability.

2.6 Confirmation of the Correctness of the Calibration Curve

According to the selected measurement conditions, use an X-ray fluorescence instrument to measure standard samples that have the same physical form and similar chemical composition as the test sample. These standard samples cannot be used to create calibration curves, and they should cover the low, medium and high points of each element correction range. Use Formula (1) to determine whether there is a statistically significant difference between the analytical value and the certified value or the standard value.

$$|\bar{x}-\mu_0| \le \frac{1}{\sqrt{2}}\sqrt{R^2-\frac{n-1}{n}\cdot r^2+2U^2} \quad (1)$$

In the Formula, $\bar{x}$ is the average value of the measured elements in the standard sample, μ_0 is the standard values of the analyzed elements in the standard sample, r is the repeatability limit determined through the common precision test, R is the reproducibility limit determined through the common test for precision, n is the number of repeated measurements of the standard sample, U is the uncertainty of the determined values of the analyzed elements in the standard sample.

3. Results and Discussion

3.1 XRD Phase Analysis of Nickel–Cobalt–Manganese Lithium Oxide

In the fusion method, in order to avoid forming low melting point alloys between metal elements and the platinumor gold which is in the Pt–Au crucible during heating and melting. If this phenomenon occurs will lead to corrosion or melting through of the Pt–Au crucible, and so the phase morphology of the sample determines whether pre-oxidation treatment is required. Therefore, the existing NCM 811-typenickel–cobalt–manganese lithium oxides tandard sample is analyzed by X-ray Diffraction (XRD). By XRD analysis, the lithium nickel-cobalt-manganese Li (Ni, Co, Mn)O_2, and no other phases are detected (Figure 1), All of the mare oxides.

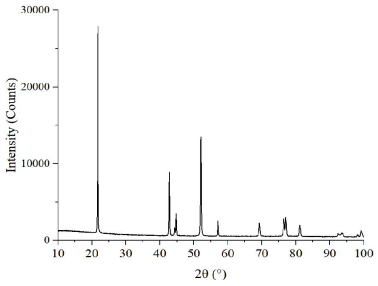

Figure 1. XRD Pattern of the NCM-811 Standard Sample

3.2 The Influence of Flux Ratio

At present, the main fluxes used for fusion sample preparation are anhydrous lithium tetraborate, lithium metaborate and mixtures of the two different proportions. In this experiment, mixed fluxes with lithium tetraborate to lithium metaborate ratios of 67: 33 are used. The diameter of the Pt-Au crucible tray used in this experiment is 40mm. If the flux mass is too low (less than 7g), the glass discsample will be incompelet (Figure 2). Therefore, to ensure the integrity of the glass disc, the flux mass is set to 10g, the flux to sample ratio is set to12.5: 1, and the sample is melted at 1150 °C. During the experiment, it was found that, at this mass ratio concentration, visible green bubbles appeared on the surface of the fused disc used as the standard

sample for drawing the calibration curve (Figure 3). The sample mass reduce to 0.6g; at this ratio, the flux to sample ratio is 16.6: 1. Under the same melting conditions, a bubble-free and precipitation-free glass disc is obtained (Figure 4). The final flux-to-sample ratio is 16.6:1.

In order to further investigate the reasons for the poor dissolution, a scanning field-emission scanning electron microscope equipped with an energy-dispersive spectrometer (SEM-EDS) was used to image and analyze the composition of the standard sample melt slice with a mass ratio of 12.5:1 (Figure 5 and Figure 6).

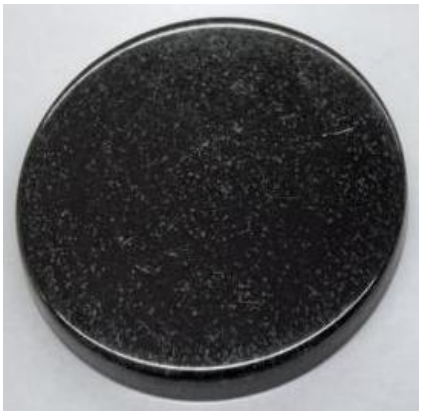

Figure 3. The Flux to Sample Ratio is 12.5: 1

Figure 2. The Incompelet Glass Disc

Figure 4. The Flux to Sample Ratio is 16.6: 1

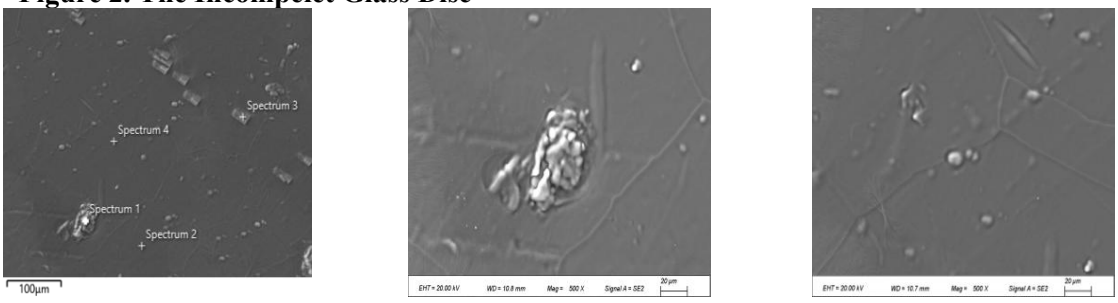

(a) **(b)** **(c)**

Figure 5. Electron Image of Sample (a: Sample Front View Picture in 100µ, b: Spectrum1 View Picture in 20µm, c: Spectrum2 View Picture in 20µm)

Through the analysis using SEM-EDS, the insoluble substances at points 1 and 3 are mainly the undissolved nickel phase, whereas at points 2 and 4, the contents of nickel, cobalt, and manganese are relatively uniform, indicating that the dissolved portion is homogeneous. By consulting relevant books and other literature, nickel oxide is known to possess a very stable rock-salt-type crystal structure and has a melting point of approximately 1955 °C. However, the fluxes commonly used in the fusion method—such as lithium tetraborate and lithium metaborate—typically melt within a temperature range of 1000 °C to 1200 °C. Within this temperature range, the thermodynamic energy of the melt is insufficient to fully disrupt the crystalline lattice of nickel oxide, making complete dissociation and incorporation into the glassy melt difficult within a short time. Therefore, optimizing the flux composition and reducing the nickel oxide content can address the issue of incomplete nickel dissolution.

3.3 Mathematical Model and Calibration

The self-made standard samples with different concentration levels were analyed determined under the instrument operating conditions listed in Table 1. The standard concentrations of the elements are plotted on the x-axis, and the corresponding fluorescence intensities are plotted on the y-axis to establish a calibration curve, it is generally expressed in the form of a quadratic equation or a linear equation, as shown in Formula (2).Where xi is the uncorrected mass

fraction (%) of the analyzed element i, Ii is the X-ray fluorescence intensity (kcps) of element i, and a, b, and c are the corresponding coefficients. When the calibration equation is linear, a equals 0.

$$X_i = aI^2{}_i + bI + c \quad (2)$$

There is significant spectral line overlap interference among Mn, Co, and Ni, which is the main source of matrix interference in XRF analysis of ternary cathode materials. The energy intervals between the main peaks are not extremely large; however, the main peaks do not overlap each other and instead interfere indirectly via secondary characteristic lines (e.g., Kβ). The most significant interference arises from the Co Kβ line overlapping with the Ni Kα line. NCM samples must therefore be corrected using a matrix correction algorithm. By employing the built-in interference coefficients of the SuperQ instrument software—as well as the overlap coefficients for Co–Ni and Mn–Co—the Kβ tailing contributions from adjacent elements are automatically subtracted. For each element, the empirical coefficient method is adopted, and the final calibration is performed according to Formula (3).In this formula, Ci represents the content (concentration) of the analytical element i, Di is the intercept constant of the calibration curve, Ei is the slope constant of the calibration curve. Ri represents the measured intensity (relative intensity) of the analytical element i. αij is the absorption (or influence) coefficient of the coexisting element j on the analytical element i. Cj is the content (concentration) of the coexisting element j.

$$C_i = D_i + E_i \cdot R_i \cdot (1 + \sum a_{ij} \cdot C_j) \quad (3)$$

The fitting curve is evaluated based on the combined root-mean-square (RMS) error and the K factor, and calibration curves for each element are established. The linear relationships for each element are shown in Figure 7. As can be seen from the figure, in this condition, the linear relationship of the nickel, cobalt and manganese elements is relatively good.

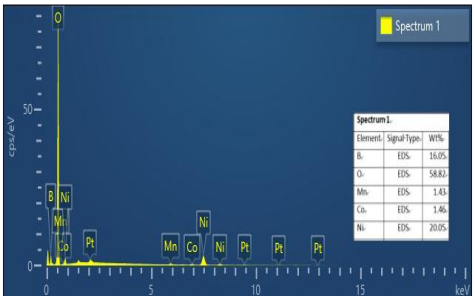

(a) Component of Spectrum 1

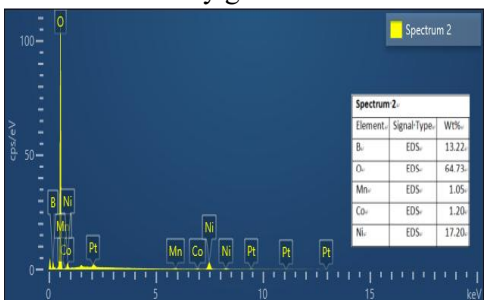

(b) Component of Spectrum 2

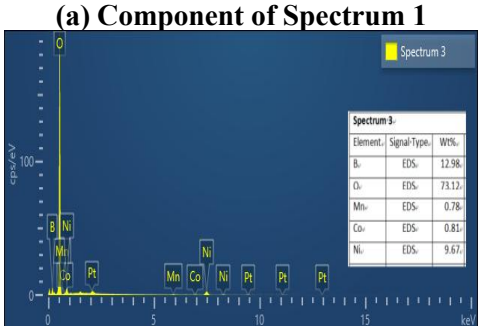

(c) Component of Spectrum 3

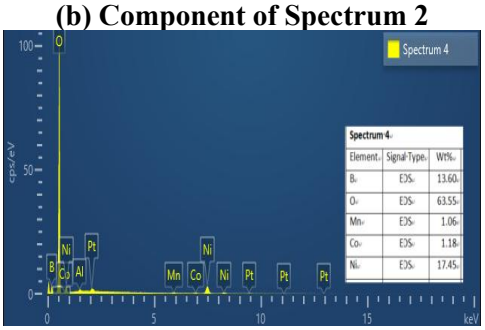

(d) Component of Spectrum 4

Figure 6. Result of Electron Analysis Component

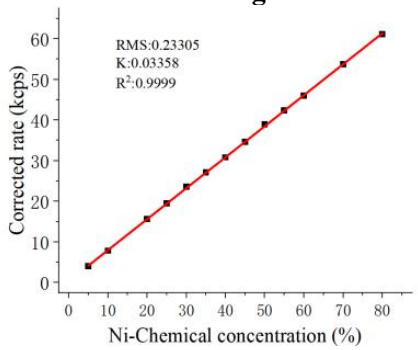

(a) Standard Curve Graph of Ni

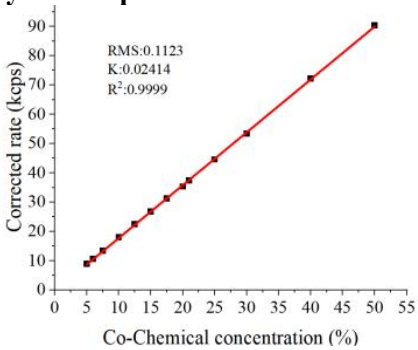

(b) Standard Curve Graph of Co

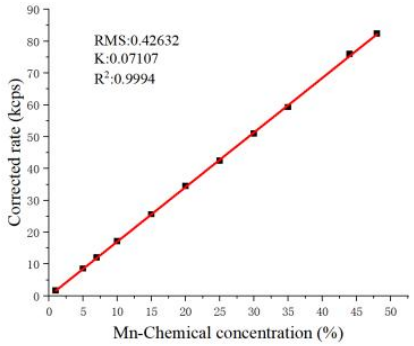

(c) Standard Curve Graph of Mn

Figure 7. Calibration Diagrams of Each Element

3.4 Precision Experiment

In the ternary nickel-cobalt-manganese lithium material, the content of nickel, cobalt and manganese is 10-60%, which belongs to the major elements. The method detection limit (LLD) is generally only applicable to trace impurity elements (at the ppm level); for high-content major elements, the detection limit is not considered, and only the precision and matrix interference correction are concerned. Different concentration gradients of nickel-cobalt-manganese oxide sample were selected. And the fused sample was prepared seven times for analysis, and the mean value and relative standard deviation (RSD) were calculated. The results are shown in Table 3.As shown in Table 3, the relative standard deviation of the determination results for each element is less than 0.30%, indicating that the method is reproducible.

Table 3. Results of Precison Experiment (%)

Sample	Element	Mean%	SD%	RSD%
1	Ni	47.440	0.067	0.14
	Co	6.334	0.013	0.20
	Mn	5.426	0.009	0.17
2	Ni	36.360	0.041	0.11
	Co	11.823	0.029	0.24
	Mn	11.386	0.017	0.15

3.5 Accuracy Experiment

A accuracys experiment was conductedusing 811-type lithium nickel-cobalt-manganese oxide reference material, and the test results are shown in Table 4. As shown in the table, the measured values agree well with the certified values of the reference material within its certified uncertainty.

Table 4. Results of Accuracy experiment (%)

Sample	Ni	Co	Mn
Standard value	47.50±0.12	6.37±0.04	5.29±0.06
Measurement value	47.61	6.36	5.33

3.6 Method Comparison

Select representative samples and measure them using different methods. Compare the results to verify the accuracy of the proposed method. First, for samples with high nickel content, the gravimetric method is used. The sample is dissolved in hydrochloric acid, and in a slightly alkaline medium, citric acid serves as a masking agent to form a red complex precipitate. After standing, the precipitate is filtered and dried to constant weight, and the nickel content is calculated. Second, cobalt and manganese are determined by ICP-OES. The sample is dissolved in hydrochloric acid and diluted to a specified volume. The concentrations are quantified using inductively coupled plasma optical emission spectrometry, and the mass contents are calculated based on the sample mass and the final solution volume. Finally, nickel, cobalt, and manganese are simultaneously determined using the method developed in this study. The detection results were analyzed using one-way analysis of variance (ANOVA, F-test) and the independent-samples t-test for mean comparison. Using Formula (4) for variance comparison, at a significance level of $\alpha = 0.05$ and referring to the one-tailed F-distribution table, we obtain $F(8, 4) = 3.84$. As shown in Table 5, all calculated F-values are less than $F(8, 4)$, indicating no statistically significant difference in variances between the two methods. When the variances of the measurement results from the two methods are not significantly different, the means can be compared. Using Formula (5), the t-statistic was calculated and compared against the critical t-value.

$$F = \frac{S^2_1}{S^2_2} \tag{4}$$

$$t = \frac{|\bar{x}_1 - \bar{x}_2|}{\sqrt{\frac{(n_1-1)S^2_1+(n_2-1)S^2_2}{n_1+n_2-2} \times \frac{n_1+n_2}{n_1 n_2}}} \tag{5}$$

In the above formula, S^2_1 is the larger variance value; S^2_2 is the value with a smaller variance; $\bar{x}_1$, $\bar{x}_2$ and are the average values of the measurement results obtained by the two methods; n_1, n_2 and are the number of measurements for each method.

When the significance level $\alpha = 0.05$ and the degrees of freedom $df = n_1 + n_2 - 2$, the critical two-tailed t-value is obtained from the t-distribution table as $t(0.05, 10) = 2.228$. As shown in Table 5, the calculated t-statistic is less than $t(0.05, 10)$, indicating that there is no statistically significant difference between the

experimental method and ICP-AES, and thus the proposed method demonstrates good accuracy and reliability.

Table 5. Results of Different Methods (%)

Sample	Element	XRF		Weight		F	t
		Measurement value	Variance	Measurement value	Variance		
1#	Ni	40.94	0.011	41.02	0.008	1.74	1.47
2#	Ni	58.48	0.017	58.45	0.018	1.17	0.41
Sample	Element	XRF		ICP-OES		F	t
		Measurement value	Variance	Measurement value	Variance		
1#	Co	9.67	0.0034	9.61	0.0036	1.14	1.64
2#	Co	2.89	0.0033	2.88	0.0038	1.37	1.63
1#	Mn	11.95	0.0003	12.09	0.0012	2.24	0.69
2#	Mn	1.24	0.0003	1.29	0.0003	1.40	0.26

4. Conclusion

Regarding the demand for rapid and accurate quantitative analysis of nickel, cobalt and manganese in lithium nickel-cobalt-manganate oxide battery materials, a fused sample preparation X-ray fluorescence spectrometer method was established. A mixed flux of lithium tetraborate and lithium metaborate, along with lithium oxide matrix matching, enables the preparation of transparent glass discs suitable for analysis via high-temperature fusion. Standard reference materials of nickel oxide, cobalt tetroxide, manganese dioxide, and lithium oxide—prepared at well-defined concentration gradients—were used to construct the calibration curve. The method was applied to analyze a certified reference material of lithium nickel–cobalt–manganese oxide (NMC). The measured values agreed well with the certified values. The relative standard deviation (RSD) for each element was less than 0.3%, demonstrating that the method meets the precision requirements for routine analysis of NMC materials under repeated measurements.

Acknowledgements

This work was supported by R&D Project of High-Power Wavelength Dispersive X-ray Fluorescence Spectrometer.

References

[1] Zhang Z Y, Bao X J, Xie S Z. Current status and suggestions on standardization construction of composition analysis and performance testing of cathode materials for lithium-ion batteries. Industrial Minerals & Processing, 2024, 53(06): pp.20-32

[2] Nadeem R, Karma M. A, Khalid A, et al. Biomass derived materials for sustainable lithium batteries: A comprehensive review on recent trends, challenges and prospects. Journal of Energy Storage, 2026, 153: pp.120965.

[3] Feng Y T, Cui P Y, Lin Y, et al. Extraction and separation of manganese and cobalt from the leaching solution of cathode materials of waste lithium batteries. Chinese Journal of Environmental Engineering, 2023, 10(17), pp.3367-2273.

[4] Tirath R, Kuppam C, Naresh A K, et al. Recycling of cathode material from spent lithium-ion batteries: Challenges and future perspectives. Journal of Hazardous Materials, 2022, 429: pp.128312.

[5] Syra M, Murillo N.T. S, Gustavo T.M. S, et al. Super Ni-rich and Co-poor $LiNi_xCo_yMn_{1-x-y}O_2$, $LiNi_xCo_yAl_{1-x-y}O_2$, and $LiNi_xCo_yMn_zAl_{1-x-y-z}O_2$ ($x \geq 0.85$) based cathodes for lithium-ion batteries: A review on emerging trends, recent developments, and future perspectives. Journal of Energy Storage. 2024, 96: pp.112612

[6] Li Y Y, Xi R H, Lan Z W, et al. Research progress on $LiNi_xCo_yAl_{1-x-y}O_2$ cathode material with high Ni. New Chemical Matertals. 2022, 5(10): pp.57-62

[7] Guo F D, Zhang B. Progress and prospect of transition metal compound cathode materials with stable metal ion storage effect in various battery systems. Green Energy & Environment 10(2025): pp.1692-1726

[8] Joey C Y, Jung P C S, Zhang J J. A review of recycling spent lithium-ion battery cathode materials using hydro-metallurgical treatments. Journal of Energy Storage, 2021, 35:pp.102217.

[9] Yu D W, Huang Z, Makuza B, Guo X Y, Tian Q H. Pretreatment options for the recycling of spent lithiumion batteries: a comprehensive review. Minerals En-gineering, 2021, 173: pp.107218.

[10] Lim D A, Shin Y K, Hong S J, et al.

Cathode Electrolyte Interphase-Forming Additive for Improving Cycling Performance and Thermal Stability of Ni-Rich $LiNi_xCo_yMn_{1-x-y}O_2$ Cathode Materials. ACS applied materials & interfaces, 2022, 14(49): pp.54688-54697

[11] Arif A, Xu M, Rashid J, et al. Efficient Recovery of Lithium Cobaltate from Spent Lithium-Ion Batteries for Oxygen Evolution Reaction. Nanomaterials, 2021, 11(12): pp.11123343

[12] Li J, Liang Y W, Li W, Ye F, et al. Research Progress on Surface Modification of High-nickel Ternary Cathode Materials for Lithium-ion Batteries. Zhengzhou Univ. (Nat.Sci.Ed.), 2024, 56(03): pp. 44-51.

[13] Zeng Y, Deng J W, Zhang J Y. Determination of Content of Zr Doping in $LiNi_xCo_yMn1_{-x-y}O_2$. Guangzhou Chemical Industry, 2017, 45(22): pp.111-113.

[14] Huang P W, Sun P G, Chen X, et al. Research Progress of $LiNi_xCo_yMn_{1-x-y}O_2$ Ternary Cathode Materials, Shandong Chemical industry, 2021, 50: pp.104-122.

[15] Armstrong A R, Robertson A D, Bruce P G. Structural transformation on cycling layered $Li(Mn_{1-y}Co_y)O_2$ cath-ode materials. Electrochimica Acta, 1999, 45(1-2): pp. 285.

[16] A. Leknizi, R. Masrour, Xu L. Investigation of the electrochemical, structural, thermodynamic, and thermoelectric properties of $LiNiO_2$ cathode material for Li-Ion batteries: an Ab initio calculations. Journal of Materials Science. 2026, 61(15):pp.10865

[17] Yu F K, Xu X C, Guo Y P. Recovery of metal ions in lithium iron phosphate powder and lithium nickel-cobalt-manganate powder by electrochemical oxidation. Separation and Purification Technology. 2024, 344: pp.127134

[18] Luo H X, Su C F. Determination of Lithium, Nickel, Cobalt and Manganese in Waste Secondary Battery by Inductively Coupled Plasma Optical Emission Spectrometry. Chinese Journal of Inorganic Analytical Chemistry, 2020, 10(01), pp.49-53.

[19] Wu J, Cui X G, Wu J M, et al. Determination of Lithium Borate, Lithium Carbonate, Manganese Dioxide, Cobalt Tetroxide and Nickel - cobalt Manganese of 13 Impurity Elements by Inductively Coupled Plasma Emission Spectrometry. Shandong Chemical industry, 2020, 49(06), pp.90-92.